Insight in thermal and fluid-dynamic properties of ribbed ducts by means of a novel clustering method

Insight in thermal and fluid-dynamic properties of ribbed ducts by means of a novel clustering method

Damiano FUSTINONI, Federica VIGNATI, Pasqualino GRAMAZIO, Luigi VITALI and Alfonso NIRO

Dipartimento di Energia, Politecnico di Milano, Milan, Italy

E-mail: alfonso.niro@polimi.it

Abstract. The analysis of experimental results on heat transfer by forced convection in diverse ribbed ducts showed that different geometries lead to comparable thermal and fluid-dynamic performances. Moreover, no evident layout has been observed in data, and therefore a statistical clustering analysis is performed to detect the rationale, if any, underlying experimental results. A novel, ad-hoc developed technique is used to disengage the clustering from the data scaling and to account for the measurement uncertainty, consisting of an agglomerative procedure, based on the definition of dynamically-changing bounding boxes, whose size depends on the Nusselt number and the pumping power. Additional informations, such as the the relevance of the diverse geometric parameters and the persistence of similarity among configurations over a range of operating conditions, can be retrieved by means of the developed technique. The described method is applied to a large dataset, obtained during an experimental campaign carried on at ThermALab of Politecnico di Milano, aimed at identifying the Nusselt number and the friction factor for diverse-rib configurations in a large-aspect ratio channel with low-Reynolds flows. The considerations originated from of the results of the clustering analysis suggest the existence of an underlying structure, pointing to a possible unique parameter, termed "generalized blockage", which is possibly able to describe the global effect of the ribs geometry on forced convection.

1. Introduction

Heat transfer enhancement in forced convection is a primary-relevance problem in both industrial and scientific research for two main reasons: the first one consists in the wide variety of applications, like solar air heaters, gas-turbine blade cooling, plate-fin compact heat exchangers and electronic components [1, 2]. The second reason lies in the large number of complex phenomena which contribute to determining the performances of each configurations. For half century, corrugated heat transfer surfaces have raised a paramount interest, since they proved to be able to optimize the trade off between effectiveness and compactness of the devices. Moreover, since the heat transfer coefficient is known to depend on the flow turbulence intensity, corrugations can promote an early departure from laminar conditions and interrupt the boundary layer growth even in configuration where only low Reynolds numbers could be attainable [3–7]. Eventually, all these advantages come at an affordable cost [8–11].

Plenty of numerical and experimental studies have been performed so far on ribbed channels, which point to their effectiveness, but also highlight that each geometric factor influences both the thermal and the fluid-dynamic performances. Therefore, a very large number of possible configurations may be devised, showing a large dispersion of the results with respect

to the controlled variables (e.g. Reynolds number, friction factor, convective heat transfer coefficient, ...) and, furthermore, no apparent underlying structure. Moreover, past works also demonstrated that different geometries may often lead to comparable performances [12–18].

In most heat transfer problems, the approach to the synthesis of experimental or numerical data is achieved by means of statistical techniques consisting in data regression based on, e.g., least squares or interpolations with known functions. This approach provides handful correlations, but it does not allow to retrieve additional informations on the possible reasons which determine the mutual influence between the factors (geometrical features and operational conditions) and the effect (the Nusselt number). Conversely, this second approach is still little adopted to study heat transfer, and therefore a statistical analysis is performed on experimental data in this work, to explore the similarity among different configuration and possibly detect a rationale, if any. Statistical clustering consists in classifying a number of so-called "multivariate data", i.e., identified by a number of diverse parameters, by defining some sets depending on similarities among their members [19]. The goal of this work is to allocate each rib-geometry configuration to a set (the so-called "cluster"), together with other configurations which produce comparable thermal and fluid-dynamic performances.

The adopted procedure consists in the so-called "agglomerative" method, that is an iterative procedure which starts with a list of the single configurations and, at each iteration, merges two elements into a new cluster. At the beginning no cluster exists, but after the first iteration any two elements, i.e., either two configurations, or two clusters, or one configuration and one cluster, can be merged together. The process terminates when all the data have been gathered into a single cluster. Unfortunately, these methods suffer from non-uniqueness, since the criterion adopted to select the elements to be merged depend on a number of arbitrarily-chosen parameters [20–22].

To fill this gap, a novel method was formulated and implemented at ThermALab of Politecnico di Milano, which overcomes the arbitrariety of previous clustering techniques and may also deal with measurement uncertainty. The method, that we termed "dynamic", is then applied to the large database obtained studying the thermal characteristics of forced flow through a rectangular channel with ribs arranged in a large variety of configurations, that has been carrying on for several years at the ThermALab of Energy Department of Politecnico di Milano [23–26]. The final goal is to compare overall performance data in the perspective of assessing whether comparable performances can be achieved using different rib geometries, to detect the most relevant geometric features in heat transfer enhancing.

2. Description of the method

The experimental facility, which is also described in [27], consists in a rectangular duct characterized by an aspect ratio of 10. Tables 1 and 2 summarize the features of the channel and ribs, respectively. All the considered ribs have square cross section with different side length, pitch-to-side ratio, design and layout. Not all the possible combinations of parameters have been explored, resulting in an overall number of geometric configurations of 58, including the smooth channel, used as reference. Some examples of rib configurations are sketched in figure 1.

Table 1. Main channel geometric parameters.

Channel height, h	12.0 mm
Channel length, L	880.0 mm
Channel width, w	120.0 mm
Hydraulic diameter, D_h	21.82 mm

Table 2. Main ribs geometric parameters. All the ribs have square section.

Rib section side, s	2 mm, 4 mm
Pitch-to-side ratio, p/s	10, 20, 40
Rib design, d	linear (tilted of 45°, 60°, 90°), continuous V-shaped, broken V-shaped. V-shaped ribs are 60°-tilted.
Ribs layout, l	aligned, staggered, crossed (for linear ribs); upstream, downstream or mixed (for continuous and broken V-shaped)

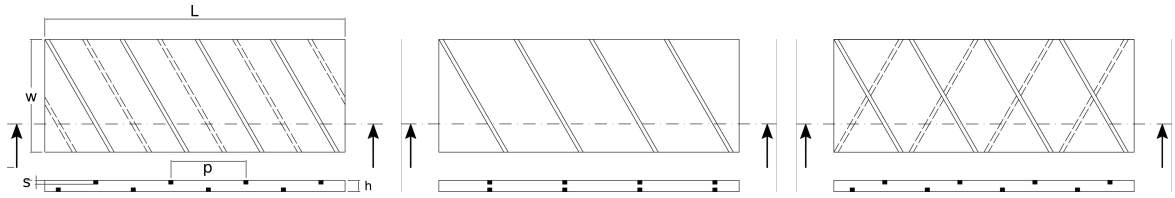

(a) Linear 60° tilted, staggered configuration

(b) Linear 60° tilted, aligned configuration

(c) Linear 60° tilted, crossed configuration

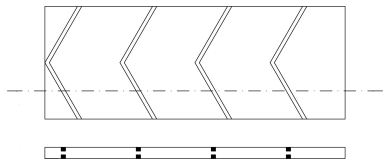

(d) Continuous V-shaped upstream, aligned configuration

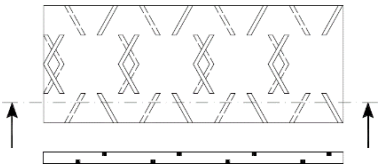

(e) Broken V-shaped, mixed configuration

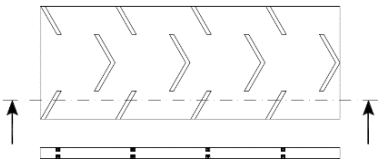

(f) Broken V-shaped downstream, aligned configuration

Figure 1. Sketches of some investigated configurations: (a) linear staggered, (b) linear aligned, (c) linear crossed, (d) V-shaped pointing upstream (the flow is from left to right), (e) V-shaped broken with mixed layout, (f) V-shaped broken pointing downwards. The ribs in all the depicted configurations are tilted of 60° with respect to the channel axis. The thickness and the pitch indicated in (a) are indicative.

The duct is operated with the lower and upper walls at fixed temperature, while the side walls are adiabatic. Air flow rates are varied for Reynolds numbers (defined over the hydraulic diameter, the bulk velocity and the kinemati viscosity) $\mathrm{Re_D}$ ranging between 600 and 10000.

In this work, the configurations will be hereafter identified by means of an alphanumeric code which summarizes the rib geometric features. The first series of symbols describes the design: linear, continuous V-shaped or broken ribs are identified by the tilt angle, the letter V and the series "3D-V", respectively. The second substring contains the initial letters of the layout name. The third and the fourth series of symbols identify the pitch-to-side ratio and the side values, respectively. Only the smooth channel is identified by the full name. The final number, included between parentheses, is simply the run order of the tests, resulting in a code like, e.g., 3D-V-up-p10-s2 to identify the configuration with broken V-shaped upstream ribs, pitch-to-side ratio of 10 and side of 2 mm.

The Nusselt number Nu and the Darcy-Weisbach friction factor f_D are computed in accordance to the procedure described in [27]. The required pumping power PP is evaluated

from f_D as

$$\mathrm{PP} = \frac{\dot{m}\Delta p}{\rho} \tag{1}$$

being $\dot{m}$ the mass flow rate, Δp the pressure drop and ρ the average air density.

A three-dimensional matrix contains all the experimental results, arranged by $\mathrm{Re_D}$, Nu and PP. All data are normalized with respect to the smooth channel values of Nusselt number and pumping power, i.e., $\mathrm{Nu_0}$ and $\mathrm{PP_0}$. This choice, which is useful to determine the *improvement* on the thermal performances, or the *penalty* on the fluid-dynamic ones, turned out to be one of the most relevant reasons which determined the necessity of devising a novel clustering method,as it will be detailed in the following.

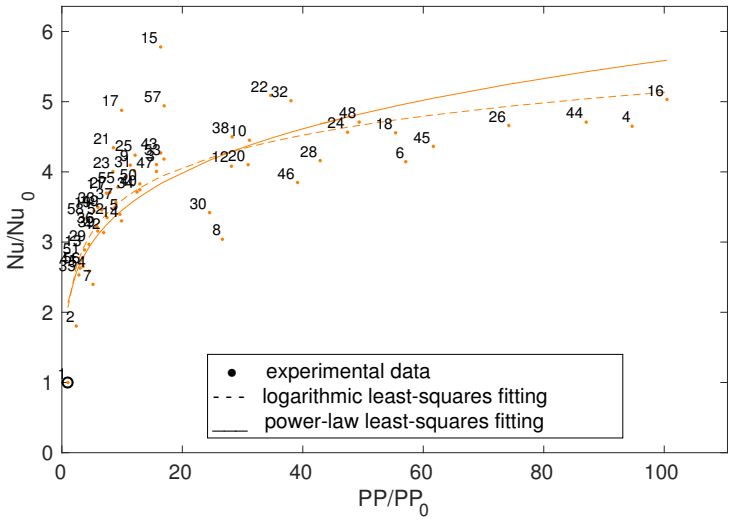

Figure 2. Experimental Nu versus PP for $\mathrm{Re_D} = 3218$. Each dot represents a different geometric configuration, ranging from 1 (smooth channel) to 58. Data are normalized with respect to the values of Nu and PP of the reference smooth channel. The full line and the dashed line represent candidate fitting curves.

A plot of Nu versus PP at $\mathrm{Re_D} = 3218$ is depicted in figure 2, where every numbered dot represents a different rib geometry. Since, in general, adjacent numbers represent configurations with comparable geometry, the plot confirms that similar thermal and fluid-dynamic performances can be obtained by adopting different geometries, and that the configurations do not present any evident underlying structure.

2.1. The statistical clustering method

For both agglomerative and divisive hierarchical clustering, it is mandatory to define some criteria to quantify the similarity among the elements of each cluster. In general, these criteria concern the following possibilities.

- A measure of the proximity between two elements (two configuration, two clusters or a configuration and a cluster), which depends only on a geometrical property, i.e., the metrics of the space which represent the data: in general, p-norms are used.
- The so-called *linkage*, i.e., a criterion to select a representative of each cluster, that is a method to associate to a set of points the coordinates of a single point only. This choice is non-trivial, as it is based on both statistical and circumstantial considerations, e.g. the physics of the problem under scrutiny.
- A scaling of the data. This point strongly influences the resulting clustering, and may depend significantly on the field of application.

Unfortunately, all these criteria are arbitrarily chosen, and lead to very different results [28–36]. All classical agglomerative techniques, hereafter defined "static" due to their definition

of the so-called *inclusion criterion* used to build the clusters, suffer systematically from this arbitrariety. At each iteration, indeed, the distances between any two elements is computed within the selected proximity measure. Then, the couple of nearest elements is selected: a new cluster is formed, which contains the two of them. The main drawback of static methods is that the clustering is very sensitive with respect to the three criteria: mainly to the scaling of the data [27,37], but also to the distance measure and to the linkage, including some additional parameters.

The novel method, called "dynamic", aims at overcoming these limitations, by adopting a similarity criterion which disengages the results from the data scaling. The proposed clustering technique is still an agglomerative, bottom-up technique, but it adopts a proper adaptive proximity measure which evolves dynamically during the cluster creation. It consists in defining a bounding box associated to each element, i.e., a region of influence, which is centered in the element: the bounding box size is non-uniform in the diverse dimensions, and moreover it is automatically and dynamically increased during the clustering procedure. For this reason, each side of the bounding box is proportional the coordinate value of the central element along that specific direction, i.e., a percentage of it. At each iteration, the coefficient of proportionality, which is therefore termed "percentage distance", is updated from zero to the final, maximum value. The similarity detection is then straightforward: if two areas of influence interact, i.e., overlap, each other, then the two associated elements are merged together to make a new cluster. For details on formulation and performance of this procedure, the reader is addressed to the original papers [27,37].

Three additional advantages derive from this formulation. On the first hand, it provides a simple solution to the so-called "ties in proximity problem" [38, 39], which rises when one element can be merged with more than one other element at the same time. Unlike most static methods, the proposed dynamic method does not require to merge exactly two elements per iteration, but it allows to merge multiple points. Secondly, the dynamic clustering allows to account for the the effect of weighting the thermo-fluid-dynamic parameters, i.e., Nu and PP, to stress the relevance of either the ribs effectiveness or the configuration efficiency. Due to the geometrical nature of the method, this result can be attained by simply stretching the aspect ratio of each bounding box along one dimension. Aspect ratios from 1 to 10 are studied in this work. Eventually, the third advantage consists in the possibility of including the effect of the measurement uncertainty [40] in the proximity measure definition, as detailed in [27].

The geometric approach, based on the intuitive definition of the bounding boxes, is straightforward and robust, but unfortunately its implementation has a much larger computational cost than the one required by standard, static clustering methods. Therefore, a new proximity measure is introduced, that will be hereafter termed "weighted asymmetric ∞-pseudometric" and indicated with the symbol d^*_∞, to include the implementation of the dynamic method in the framework of classical, more efficient clustering algorithms. If multivariate data are represented by the elements P, Q and depend on N variables in the space V (e.g., $V = \mathbb{R}^N$), this proximity is defined as

$$\begin{aligned} d^*_\infty(P,Q) &= \min_{R=P,Q}\left(\max_i\left(\lim_{w_i\to R_i}\left|\frac{P_i-Q_i}{w_i}\right|\right)\right) \\ &= \min\left(\max_i\left(\lim_{w_i\to P_i}\left|\frac{P_i-Q_i}{w_i}\right|\right), \max_i\left(\lim_{w_i\to Q_i}\left|\frac{P_i-Q_i}{w_i}\right|\right)\right) \end{aligned} \tag{2}$$

where P_i, Q_i are the values of the i-th variable making up the multivariate data (here, Nu and PP), and w_i the corresponding value of the weight, which is automatically and adaptively computed along the progress of the clustering algorithm.

The algorithm was validated over a number of toy problems [37], showing good stability and speed.

3. Results

For each combination of Reynolds number and aspect ratio, the hierarchical clustering is found and it is represented by means of a dendrogram. The dendrogram ordinate represents the increasing size of the area of influence, necessary to cluster the different configurations. This value ranges from zero (for identical configurations) to the maximum value (for the least similar configurations). Four values of bounding box aspect ratio are adopted, e.g., 1, 2, 5 and 10.

The dendrogram resulting from the dynamic clustering of data obtained for $\mathrm{Re_D} = 5353$ and unit bounding box aspect ratio is depicted in figure 3 (in blue) The dendrogram in figure 3 is rotated of 90 ° counterclockwise to fit in the page, and therefore the ordinate, representing the percentage distance, is the horizontal axis. To detect which configurations share a reasonable similarity degree for engineering considerations, a threshold value of 20% is selected, as explained in the following. Therefore, the configurations with a percentage distance lesser than or equal to 20% are merged together to form groups. The red line in figure 3 represents the threshold, i.e., the percentage distance of 20% among the configurations, which summarizes in one parameter all the effects of the multivariate data. In this perspective, all the configurations that belong to the same group have a reciprocal distance smaller than 20%, and they are indeed linked by a branch intersecting the red line. Therefore, the groups resulting from this procedure depend on both the Reynolds number and the aspect ratio of the bounding boxes.

The threshold value of 20% is chosen as a compromise between two factors. On the one hand, experimental data suffer from a measurement uncertainty which was estimated [40] to be less than 7% as discussed in [23–25]. For this reason, the threshold must be larger enough to recognize real distances between configuration pairs. On the other hand, the dendrograms analysis show that threshold value larger than 20% would decrease the selectivity of the procedure. Therefore, the validity of the proposed value of 20% is not general: if a different sensitivity is required, the threshold value should be modified.

It is observed that, when the aspect ratio of the influence area is larger than one, the result of the clustering is trivial. This is observed also for different values of threshold. Therefore, in the following, all the considerations concern the case on unit aspect ratio.

3.1. Results synthesis

For every Reynolds number, the results of the described procedure are summarized by a table of size 58x58, termed "adjacency matrices". Each row and column of the table represents one of the 58 geometric configurations. If the two configurations associated to the $j-th$ row – $k-th$ column pair of a cell belong to the same group –i.e., if their percentage distance is below 20%– the cell value is 1, otherwise it is zero. This value, hereafter termed "similarity coefficient" has a logical, boolean meaning, and, therefore, all the matrices are symmetric with unit values along the main diagonal.

All these tables provide complete informations but, unfortunately, they do not allow synthetic considerations. To obtain a deeper insight, the persistence between each pair of configurations for different Reynolds numbers is investigated. To obtain this effect, the tables computed for different Reynolds numbers are combined by means of a matrix addition, resulting in a single table. The latter, termed "aggregate table" and of size 58x58, contains integer values between 0 and 8 (the same number as the investigated Reynolds values). The larger the value, the more persistent the similarity between the two associated configurations. This allows not only to detect the configuration with the most robust similarity, but it is useful for applications with a high risk of operating in off-design conditions.

The observation of the aggregate table suggests that configurations with very different geometric parameters systematically may group together also for diverse Reynolds. On the contrary, other configurations with similar geometry never result in comparable performances.

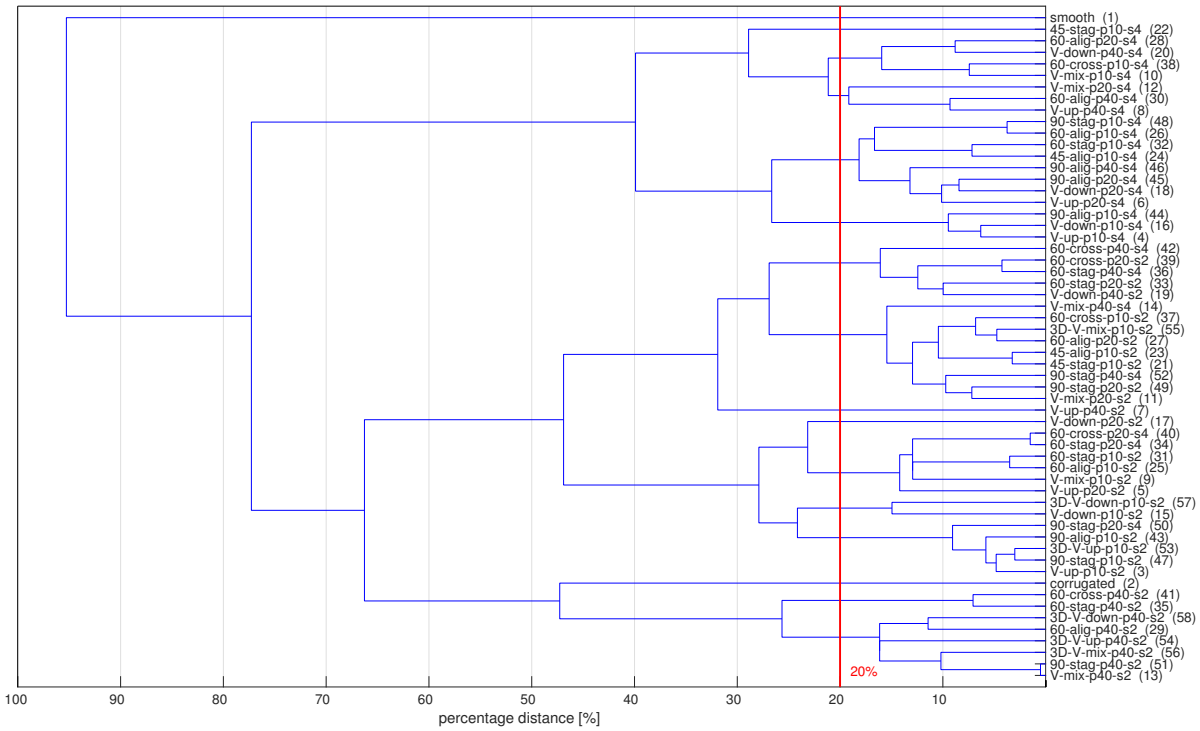

Figure 3. Dendrogram resulting from the clustering of experimental data for $Re_D = 5353$ with unit aspect ratio. The vertical red line highlights configurations with percentage distance <20%.

3.2. Application to ThermALab results

The order of rows and columns in the adjacency matrices simply represents the run-order of the experimental configurations. For this reason, the matrices rows can be arbitrarily permuted. Of course, to preserve the meaning of the adjacency and aggregated matrices, the same permutation must be applied also to the columns.

Although any permutation can be applied, some of them allow to observe a specific structure underlying the similarity coefficient and, therefore, also to derive a criterion to gain a further insight into the aggregation of the diverse geometrical configurations. The matrices rows are sorted to gather together, in horizontal bands, all the experimental configurations sharing the same value of each geometric parameter. Since each configuration is identified by the parameters side thickness, pitch-to-side ratio, design and facing (cf. table 2), four permutations are applied to the matrices rows (and, correspondingly, to the columns).

The new arrangements allow to consider the relevance of each geometric parameter on the similarity between the performances of two configurations. Indeed, the stronger one parameter influence, the more evident the block-structure of the matrices resulting from the sorting based on that parameter. Moreover, if the parameter selected to drive the sorting has a relevant influence on the similarity, within each block the larger similarity coefficients tend to approach the block main diagonal. Out of the blocks, the number of non-zero similarity coefficient is lower (ideally null) for more relevant parameters, indicating poor similarity between configurations with different values for the considered geometric parameter. Figure 4 shows two matrices resulting from the permutations of the same Reynolds-aggregated matrix: the driving parameter is the ribs side length in picture 4(a), and the ribs facing in picture 4(b). In figure 4, the lighter the cell color, the larger the numerical value therein, ranging from zero (dark orange, empty

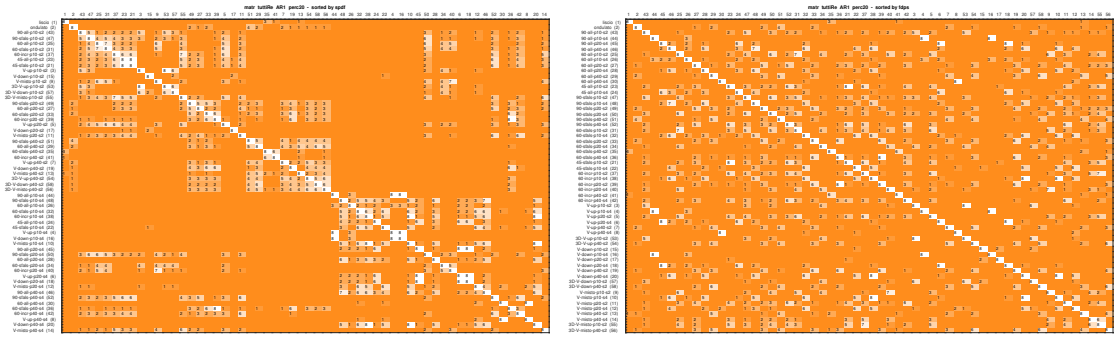

(a) (b)

Figure 4. Reynolds-aggregated matrix resulting from the dynamic clustering of data with a unit-value bounding box aspect ratio. The sorting aims at gathering configuration which share the same (a) side and (b) facing. The lighter the cell color, the larger the numerical value therein, ranging from zero (dark orange, empty cells) to eight (white cells)[1].

cells) to eight (white cells)[1]. The block structure is more evident when the sorting is performed by merging the configurations with the same side length, than for the other case, indicating the side length as a more significant parameter on the performance similarity between configurations.

In the following, 7 families of configurations are presented, as resulting from the application of the described procedure to the Reynolds-aggregated matrix with unit-value aspect ratio and threshold value of 20%. This combination of aspect ratio and threshold value is selected, as it results to be the most significant one.

(i) V-down-p40-s4 (20), 60-cross-p10-s4 (38), V-mix-p10-s4 (10)
(ii) V-down-p20-s4 (18), 90-alig-p20-s4 (45), V-up-p20-s4 (6)
(iii) V-down-p10-s4 (16), 90-alig-p10-s4 (44), V-up-p10-s4 (4)
(iv) V-up-p40-s4 (8), 60-alig-p40-s4 (30)
(v) 45-stag-p10-s2 (21), 45-alig-p10-s2 (23)
(vi) V-up-p10-s2 (3), 3D-V-up-p10-s2 (53)
(vii) 60-stag-p40-s4 (36), 60-cross-p20-s2 (39)

The observation of the families detected by the research of recurring patterns in the Reynolds-aggregated matrices leads to two main considerations. The first one concerns the families identified as (i), (ii) and (iii) in the list: the average Nusselt numbers for each family are fairly close to the other ones, but the required pumping powers are very different. Moreover, the most relevant geometric parameter, i.e., the rib side, is $s = 4\,\text{mm}$ for all the configurations in families (i), (ii) and (iii), whereas the effects of facing and design are not evident in the association among families. The pitch-to-side effect appears to be controversial: all the ribs in family (iii) have $p = 10$, which becomes $p = 20$ for the ribs in family (ii). However, this trend between the pitch-to-side ratio and the decreasing pumping power is arrested, since only one configuration in family (i) has $p = 40$, opposed to the value of $p = 10$ of the others.

The second consideration concerns the stability of the seven families of configurations described above, as they are detected also by analyzing Reynolds-aggregated matrices for larger aspect ratios, the overall-aggregated matrix and aspect ratio-aggregated ones. The only exception is observed for family (vii), which is not highlighted in some isolated cases. The

[1] Due to the small size of the figures, numbers in each cell of figure 4 can be read only in the digital copy, with a suggested 4x enlargement.

systematic observation of these families, regardless of the matrix aggregation criterion and the operating conditions, confirms the stability of the clustering and suggests an underlying physical reason.

4. Conclusions

The novel, dynamical method formulated al ThermALab of Politecnico di Milano is described here and applied to research a possible criterion to classify experimental data. It is indeed observed that, while investigating the performances of ribbed ducts with different geometry used to enhance heat transfer in forced convection, quite different rib geometries may often result in similar performances, despite the lack of an evident correlation between their geometry and thermal-fluid-dynamic effects.

The method is applied to the large database obtained during a long term experimental campaign carried on at ThermALab, to identify the Nusselt number and the friction factor of low-Reynolds flows in a large-aspect ratio rectangular duct. The advantages of the proposed method consists in a large robustness of the results, in the possibility of accounting for the measurement uncertainty and in the possibility of giving more relevance to either Nu or PP, depending on the applications. A fast, memory saving algorithm is formulated, which does not require additional cost, if compared to classical techniques.

The analysis of the resulting clusters points to the existence of some families of configurations which presents comparable performances. Only in some cases the configurations of the same family share one or more geometric features, whereas, more unexpectedly, other configurations with similar geometries do not produce comparable results.

To observe the persistence of the similarity over a range of Reynolds numbers, a further step is performed, which allowed to identify 7 stable families of configurations.

Next step will be the definition of one single parameter, which is able to uniquely identify all the configurations which belong to each family, and, therefore, to predict the performances of a rib geometry without the need of carrying on extensive numerical or experimental campaigns.

References

[1] Webb R L 1994 *Principles of enhanced heat transfer* (New York: Winley-Interscience)
[2] Gupta S, Chaube A and Verma P 2012 Review on Heat Transfer Augmentation Techniques: Application in Gas Turbine Blade Internal Cooling *J. Eng. Sci. Tech. Rev.* **1** 57–62
[3] I.A. Popov, Y.F. Gortyshov, V.V. Olimpiev, *I. A. Popov, Yu. F. Gortyshov, and V. V. Olimpiev*, Thermal Engineering, vol. 59(1), pp. 1-12 (2012)
[4] B. Arman, T.J. Rabas, *Two-layer-model predictions of Heat Transfer inside Enhanced Tubes*, Numerical Heat Transfer, Part A: Applications, vol 25 (1994)
[5] F.J. Edwards, N. Sheriff, *The heat transfer and friction characteristics for forced convection air flows over a particular type of rough surface*, Internat. Devel. Heat Transfer, pt. 3, Ser. A, ASME, New York, pp 415-425 (1961)
[6] R.L. Webb, E.R.G. Eckert, R.G. Goldstein, *Heat transfer and friction in tubes with repeated-rib roughness*, International Journal of Heat and Mass Transfer, vol 14(4), pp 601-617 (1971)
[7] T. Ota, Y. Okawa, *Transition of the separated flow over blunt flat plates*, Bull. of the JSME, vol. 24, pp. 941-947 (1981)
[8] Han J C and Park J S 1985 Heat transfer enhancement in channels with turbulence promoters *J. Eng. Gas Turb. Power* **107** 628–35
[9] Han J C, Zhang Y M and Lee C P 1991 Augmented heat transfer in square channels with parallel, crossed, and V-shaped angled ribs *J. Heat Trans.* **113** 590–96
[10] Kukreja R T, Lau S C and McMillin R D 1993 Local heat/mass transfer distribution in a square channel with full and V-shaped ribs *Int. J. Heat Mass Tran* **36** 2013–20
[11] Gao X and Sunden B 2001 Heat transfer and pressure drop measurements in rib-roughened rectangular ducts *Exp. Therm. Fluid Sci* **24** 25–34
[12] Han J C 1988 Heat transfer and friction characteristics in rectangular channel with rib turbulators *ASME J. Heat Trans.* **110** 321–28

[13] Park J S, Han J C, Huang Y, Ou S and Boyle R J 1992 Heat transfer performance comparisons of five different rectangular channels with parallel angled ribs *Int. J. Heat Mass Tran.* **35** 2891–903
[14] Han J C and Park J S 1988 Developing heat transfer in rectangular channels with rib turbolators *Int. J. Heat Mass Tran.* **31** 183–95
[15] Han J C, Ou S, Park J S and Lei C K 1989 Augmented heat transfer in rectangular channels of narrow aspect ratios with rib turbolators *Int. J. Heat Mass Tran.* **32** 1619–30
[16] Liu J, Gao J and Gao T 2012 Forced convection heat transfer of steam in a square ribbed channel *J. Mec. Sci. Tech.* **4** 1291–98
[17] Liu J, Gao J, Gao T and Shi X 2013 Heat transfer characteristics in steam-cooled rectangular channels with two opposite rib-roughened walls *App. Therm. Eng.* **50** 104–11
[18] Choi E Y, Choi Y D, Lee W S, Chung J T and Kwak J S 2013 Heat transfer augmentation using rib-dimple compound cooling technique *App. Therm. Eng.* **51** 435–41
[19] Johnson R A and Wichern D W 1992 *Applied multivariate statistical analysis* (NJ: Englewood Cliffs) vol. 4
[20] Anderberg M R 1973 *Cluster analysis for applications* (New York: Academic Press, Inc)
[21] Rand W M 1971 Objective criteria for the evaluation of clustering methods *J of the Am. Stat. Ass.* **66.336** 846–50
[22] Davé R N and Krishnapuram R 1997 Robust clustering methods: a unified view *Fuzzy Systems, IEEE Trans.* **5.2** 270–93
[23] Fustinoni D, Gramazio P, Colombo L and Niro A 2015 Heat transfer characteristics in forced convection through a rectangular channel with broken V-shaped rib roughened surface *J. of Phys.: Conf. Series* **655** 012060
[24] Fustinoni D, Gramazio P, Colombo L and Niro A 2014 Heat Transfer characteristics in forced convection through a rectangular channel with V-shaped rib roughned surfaces *15th Int. Heat Transf. Conf.*, Kyoto
[25] Fustinoni D, Gramazio P, Colombo L, Niro 2012 A First average and local heat transfer measurements on forced air-flow at low Re-numbers through a rectangular channel with ribbed surfaces *Ed. Soc. Fr. de Thermique*, Paris
[26] Fustinoni D, Niro A 2010 Experimental investigation by IR-thermography of heat transfer over rib-roughned surfaces *Heat Transf. Conf.*, Washington
[27] Niro A, Fustinoni D, Vignati F, Gramazio P, Ciminà S 2016 Considerations on the thermal performances of ribbed channels by means of a novel dynamic method for hierarchical clustering *7-th Eurotherm, Kraków*
[28] Sokal RR, Sneath PHA 1963 Principles of Numerical Taxonomy *W.H. Freeman and Company* San Francisco
[29] Johnson RA, Wichern DW 1990 Applied Multivariate Statistical Analysis *Pearson Education* New York
[30] Anderson TW 1984 An Introduction to Multivariate Statistical Analysis *John Wiley & Sons* New York
[31] Rohlf FJ, Sokal RR 1962 The Description of Taxonomic Relationships by Factor Analysis *Systematic Zoology 11* **1**
[32] Day WHE, Edlesbrunner H 1985 Investigation of Proportional Link Linkage Clustering Methods *Journal of Classification* **2** 239-254
[33] Fernández A, Gómez S 2008 Solving Non-Uniqueness in Agglomerative Hierarchical Clustering Using Multidendrograms *Journal of Classification* **25** 43-65
[34] Jain AK 2010 Data clustering: 50 years beyond K-means *Pattern Recognition Letters* **31** 651-666
[35] Kleinberg J 2002 An impossibility theorem for clustering *Advances in Neural Information Processing Systems* **15** MIT Press, Boston 446-453
[36] Fortunato S 2010 Community detection in graphs *Physics Reports* **486** 75-174
[37] Vignati F, Fustinoni D, Niro A 2018 A novel scale-invariant, dynamic method for hierarchical clustering of data affected by measurement uncertainty *Journal of Computational and Applied Mathematics* **344** 521-531
[38] MacCuish J, Nicolaou C, MacCuish NE 2001 Ties in Proximity and Clustering Compounds *J. Chem. Inf. Comput. Sci* **41** 134-146
[39] Jain AK, Dubes RC 1998 Algorithms for Clustering Data *Prentice Hall Advanced Reference Series: Englewood Cliffs*, NJ
[40] Moffat R J 1988 Describing the uncertainties in experimental results *Exp. Therm. Fluid Sci.* **1** 3–17